Int J Adv Manuf Technol (2009) 42:1052–1064
DOI 10.1007/s00170-008-1662-7

ORIGINAL ARTICLE

Optimization of machining parameters using magnetic-force-assisted EDM based on gray relational analysis

Yan-Cherng Lin · Ho-Shiun Lee

Received: 17 November 2007 / Accepted: 8 July 2008 / Published online: 31 July 2008

Abstract This work developed a novel process of magnetic-force-assisted electrical discharge machining (EDM) and conducted an experimental investigation to optimize the machining parameters associated with multiple performance characteristics using gray relational analysis. The main machining parameters such as machining polarity (P), peak current (I_P), pulse duration (τ_P), high-voltage auxiliary current (I_H), no-load voltage (V), and servo reference voltage (S_V) were selected to explore the effects of multiple performance characteristics on the material removal rate, electrode wear rate, and surface roughness. The experiments were conducted according to an orthogonal array L18 based on Taguchi method, and the significant process parameters that affected the multiple performance characteristics of magnetic-force-assisted EDM were also determined form the analysis of variance. Moreover, the optimal combination levels of machining parameters were also determined from the response graph and then verified experimentally. The multiple performance characteristics of the magnetic-force-assisted EDM were improved, and the EDM technique with high efficiency, high precision, and high-quality surface were established to meet the demand of modern industrial applications.

Y.-C. Lin (✉)
Department of Mechanical Engineering,
Nankai University of Technology,
Caotun, Nantou 54243, Taiwan
e-mail: ycline@nkc.edu.tw

H.-S. Lee
Graduate Institute of Engineering Technology,
Chungchou Institute of Technology,
Yuanlin, Changhau 51003, Taiwan

Keywords Magnetic-force-assisted EDM · Gray relational analysis · Material removal rate · Electrode wear rate · Surface roughness · Multiple performance characteristics

1 Introduction

Recent years have seen a rapid development of manufacturing techniques in order to fit the demands of industrial applications. In addition, the multi-variety and small batch product have become the major trend. For fitting this development of modern manufacture and the market lead for commercial purpose, industrial producers must shorten the time-to-market duration of a new product. Consequently, to develop a new process with high efficiency, high precision, and reliability is a crucial point to support the development of modern industrial applications. Indeed, one of the non-conventional processes like electrical discharge machining (EDM) is extensively applied in mold- and die-making industries. According to the survey of Fallbohmer et al. [1], almost 90% of mold and die makers employed EDM process to finish the products in USA, Germany, and Japan. Therefore, the EDM technique is an important approach for mold- and die-making industries to fabricate their products with superior performance and accuracy. During EDM process, the tool electrode and the workpiece are separated by a small gap (about 5–100 μm). The gap width between workpiece and electrode is extremely small, so the machining debris resulting from the EDM process is difficult to remove out of the machining gap. The state of dielectric fluid isolation was difficult to recover completely during a quite short interval when the debris clogged in the machining gap became enormous. As a result, there is a high chance of forming abnormal electrical discharges in the machining zone during EDM process. In general, the

stability of EDM process significantly affects the machining characteristics. When the machining debris is expelled from the machining gap in a fast and easy way, there will be an obvious improvement in the stability of EDM process. Therefore, upon attaching magnets to conventional EDM machine, the machining zone would generate magnetic forces to drive the suspending debris expelled from the discharge gap. Since the debris stacked on the machining zone can be reduced, the machining condition becomes more stable, leading to an improvement in machining performance.

Several researchers have focused their efforts on magnetic force applications to promote the manufacturing technique during the last decade [2–12], and the beneficial effects of the magnetic force process were verified experimentally. Those investigations almost concentrated on developing feasible and reliable magnetic abrasive media. The experimental results suggested that the magnetic force process adopting magnetic media was one of the most promising processes. The magnetic abrasive processes would be regarded as attractive and excellent alternative processes for surface finishing. Kim and co-workers [13] investigated the effect of a magnetic field on electrolytic finishing process associated with the migration of ions. Their findings revealed that the migration path of the electrolytic ion could be changed by the magnetic field. In addition, the surface finishing effects could be improved to obtain a high quality of surface integrity effectively and quickly. De Bruijn et al. [14] reported that the magnetic field could significantly improve the gap cleaning. Nevertheless, reports associated with the use of magnetic force in the EDM process to improve the machining characteristics are relatively scarce in the literature.

The ability to expel debris out of the machining gap was a crucial point to maintain the stability of EDM progress and to improve the machining efficiency and surface quality. Several researchers have investigated the effects of dielectric flushing methods and explored the ejection mechanisms of machining debris in the EDM process [15–19]. For improving the debris expulsion and to prevent the clogging of debris in the machining gap, ultrasonic vibration mechanisms were added through electrodes (either tool electrode or workpiece) and dielectric fluid to solve the problem of debris accumulation and to maintain the stability of EDM progress [20–23]. Their research findings suggested that decreasing the debris accumulated on the machining zone had an important benefit to promote the machining efficiency in the EDM process. Furthermore, the added abrasives that acted as the machining media for the combined process of EDM with ultrasonic machining (USM) can be regarded as the surface strengthening agents. The added abrasives could be transferred to the machined surface to gain the effect of surface modification through the ionization of discharge column during the process [24]. As a result, the combined process of EDM with USM had the potential to prevent the accumulation of debris, which improved the machining efficiency, and to modify the machined surface. However, to design a set of USM equipment for wide machining application was intensively constricted. Besides, the degree of tool fastened on the USM system was rigorous. Thus, to construct a combined process of EDM with USM for various workpiece dimensions in a convenient, effective, and economic way was a real challenge. Especially, the EDM process in mold and die applications with large projection area is required urgently. Nevertheless, the debris expulsion in such a situation was relatively severe during EDM. An innovative technique for overcoming such a restriction in the EDM process is highly required. Consequently, a magnetic force device was attached to the EDM machine to facilitate and to expel the machining debris from the machining zone, which required a comprehensive study.

Gray theory has been widely used in engineering analysis, and it reveals the potential to solve the setting of optimal machining parameters associated with a process with multiple performance characteristics [25–33]. Therefore, the approach of gray relational analysis will facilitate the development of a novel process to fit the demands of industrial applications. In this investigation, the effects of EDM essential parameters such as machining polarity (P), peak current (I_p), auxiliary current with high voltage (I_H), pulse duration (τ_p), no-load voltage (V), and servo reference voltage (S_v) were varied to determine their effects on material removal rate (MRR), electrode wear rate (EWR), and surface roughness (SR). An L18 orthogonal array based on the Taguchi experimental design method was utilized to plan the experiments in this work. In addition, the experimental data were transferred to gray relational grade and were assessed by analysis of variance (ANOVA) to determine the significant machining parameters and to obtain the optimal combination levels of machining parameters for multiple performance characteristics. Therefore, the optimal machining parameters of the magnetic-force-assisted EDM were established to achieve a sophisticated process with high efficiency and high quality of surface integrity to meet modern industrial requirements.

2 Experimental method

2.1 Experimental equipment and procedures

In this study, a transistor-controlled EDM machine with built-in capacitors in the circuit was adopted, which was a commercial-type die-sinking EDM (model Yawjet-5 manufactured by Yihawjet, Taiwan). A novel self-designed

magnetic-force-assisted device was attached to the EDM machine, so that the EDM process and the magnetic force device operated synchronously. In addition, the versatile apparatus was used to conduct a series of experiments to explore the performance characteristics of the magnetic-force-assisted EDM on SKD 61. The schematic diagram of experimental setup is shown in Fig. 1. The magnetic-force-assisted device using a rotational disk (rotational speed, 1,200 rpm) fastened with two magnets (magnetic flux density, 0.3 T) and driven by an electrical motor was just set underneath the EDM machining zone. This magnetic-force-assisted device would facilitate the machining debris expelled from the machining zone more easily and quickly. Figure 2 illustrates the action of machining debris driven by magnetic force during the process. Moreover, a fast digital oscilloscope (Tektronix TD 2014), coupled with current probe (Chauvin Arnoux E3N) and passive voltage probe (P2200), was used in the experiments to monitor the waveforms of discharge current and voltage. The discharge waveforms were utilized to explore the beneficial effects of the magnetic-force-assisted EDM compared to that of a conventional EDM. The EDM progress could be evaluated and determined through diagnosing the discharge waveforms and counting the number of effective discharge waveforms during a fixed period. The electrical discharge power supply system used in this work is an iso-energy

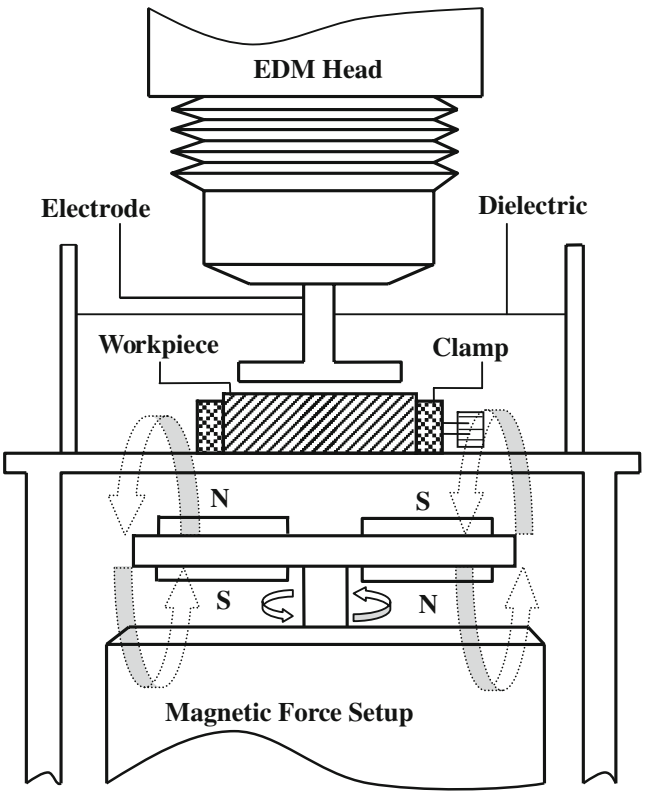

Fig. 1 Schematic demonstration of magnetic-force-assisted EDM

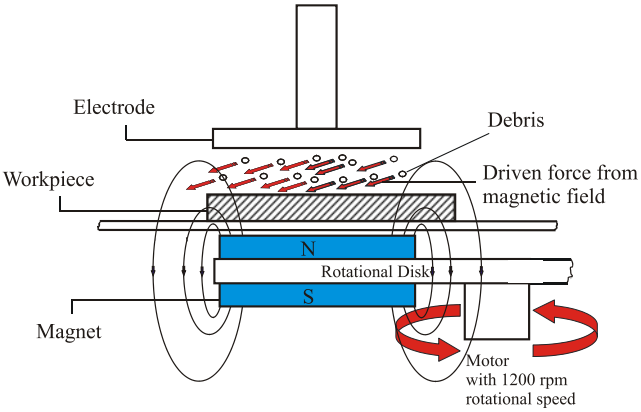

Fig. 2 Schematically diagram of the debris driven by the magnetic force in machining gap

type; the discharge waveforms could be distinguished into normal discharge, arcing, and short [34]. Since the elapsed machining time of EDM process was longer, the machining debris was aggregated in the machining gap between tool electrode and workpiece. Consequently, the debris accumulated in the machining gap would result in unstable electrical discharge as a result of arcing and shorting.

The machining characteristics such as MRR (mm^3/min), EWR (mm^3/min), and surface roughness (Ra, μm) were chosen to assess the effects of machining parameters associated with the magnetic-force-assisted EDM. The workpiece and tool electrode specimens were weighed using a precision electronic balance (Percisa XT 220A) with 0.1 mg resolution before and after each experiment to calculate the MRR and EWR. The SR was measured by a precision profilometer (Mitutoyo Surfest 4) to evaluate the surface quality of the machined surface. The value of SR was obtained by taking the average of five measurements that are stochastically acquired from the different positions of machined surface at each machining condition.

The experimental design utilized an L18 orthogonal array based on the Taguchi method (see Table 1). The L18 orthogonal array had eight columns and 18 rows, so it had 17 degrees of freedom to treat one parameter with two levels and seven parameters with three levels. Thus, eight machining parameters were assigned to the columns and the rows designated 18 experiments with various combination levels of the assigned machining parameters. In this investigation, only six machining parameters were considered with two empty columns. The orthogonality is preserved even if the two columns of the array remained empty.

The machining parameters, such as machining polarity (P), peak current (I_p), auxiliary current with high voltage (I_H), pulse duration (τ_p), no-load voltage (V), and servo reference voltage (S_v) were varied to determine their effects on the machining characteristics MRR, EWR, and SR. Table 2 presents the experimentally observed values,

Table 1 L18 orthogonal array

No	Control parameters							
	A	B	C	D	E	F	G	H
1	1	1	1	1	1	1	1	1
2	1	1	2	2	2	2	2	2
3	1	1	3	3	3	3	3	3
4	1	2	1	1	2	2	3	3
5	1	2	2	2	3	3	1	1
6	1	2	3	3	1	1	2	2
7	1	3	1	2	1	3	2	3
8	1	3	2	3	2	1	3	1
9	1	3	3	1	3	2	1	2
10	2	1	1	3	3	2	2	1
11	2	1	2	1	1	3	3	2
12	2	1	3	2	2	1	1	3
13	2	2	1	2	3	1	3	2
14	2	2	2	3	1	2	1	3
15	2	2	3	1	2	3	2	1
16	2	3	1	3	2	3	1	2
17	2	3	2	1	3	1	2	3
18	2	3	3	2	1	2	3	1

machining parameters (control parameters), and the levels of the machining parameters designed in the experiments. Moreover, the machining time of each experiment was set at 45 min in this study.

2.2 Experimental materials

The workpiece material was SKD 61 steel, which is widely used in die- and mold-manufacturing industries, with a dimension of 50×50×5 mm. The specimens were milled and ground to ensure parallelism before conducting the experiments. Table 3 presents the chemical compositions of the workpiece material. The electrode material was electrolytic copper, which is the most commonly used material in EDM industries. The electrode front face was ϕ35 mm with 5-mm thickness to conduct electrical discharges during the EDM process, and the stem diameter of the electrode was ϕ8 mm with 40-mm length to fasten on the spindle of the EDM machine. The front face of electrode against the workpiece was ground using the emery paper with mesh sizes of 600#, 800#, and 1,200# to guarantee the surface finishing and the flatness of each electrode at the same level. Table 4 shows the essential properties of electrolytic copper. In addition, kerosene (commercial grade) was employed as a dielectric fluid in this investigation.

Table 2 Experimental observed values and levels of machining parameters

Observed values	Control parameters	Levels		
Material removal rate, MRR (mm^3/min)	Machining polarity (P)	(−)		(+)
	Peak current (I_p) (A)	5	10	20
Electrode wear rate, EWR (mm^3/min)	Auxiliary current with high voltage (I_H) (A)	0.4	0.8	1.2
	Pulse duration (τ_p) (μs)	50	150	460
Surface roughness, SR (μm)	No load voltage (V) (V)	120	160	200
	Servo reference voltage (S_v) (V)	10	20	40

Table 3 Chemical compositions of SKD 61

Element	C	Si	Mn	Cr	Mo	V
wt.%	0.32–0.42	0.8–1.2	<0.5	4.5–5.5	1.—1.5	0.8–1.2

2.3 Gray analysis system theory

The gray system theory was proposed by Deng in 1982, and it is widely used for analyzing a system in which the model is uncertain or the information is incomplete. It also provides an efficient solution to complicated interrelationships among multiple performance characteristics [25, 26, 29, 30]. Therefore, the relationships between the machining performance characteristics and the machining parameters can be determined using gray relational analysis. Based on the gray theory, a system can be investigated by means of relational grade, modeling, prediction, and decision. Consequently, using gray relational analysis, the gray relational grade can be obtained to evaluate the multiple performance characteristics, so that the optimal objective of complicated multiple performance characteristics can be transferred for the optimization of a single gray relational grade.

2.3.1 Gray relational generating

Gray relational analysis adopted discrete measurements to evaluate the distance between two sequences and then explored the extent of their relationships. The sequences must have some aspects, such as comparative, invariant

Table 4 Essential properties of copper electrode

Essential properties	Descriptions
Specific gravity (g/cm^3)	8.94
Melting range (°C)	1,065–1,083
Thermal conductivity (W/m·K)	388
Specific heat (J/kg·K)	385
Electrical resistivity (Ω·cm)	1.7×10^{-6}
Thermal expansion coefficient (1/°C)	16.7×10^{-6}

scaling, and identical polarization, when they are assigned to conduct gray relational analysis. In general, if the sequence range is excessively large and the standard value is too enormous, it will induce the effect of some factors to be ignored. Moreover, when the goals and directions of the sequences are different, the relational analysis could also draw improper results. Therefore, the original data were normalized into the range between zero and one. This procedure is also called the gray relational generating. According to the performance characteristics, the sequences can be categorized to three types:

1. The-higher-the-better (HB)

$$x_i^*(k) = \frac{x_i^{(0)}(k) - \min x_i^{(0)}(k)}{\max x_i^{(0)}(k) - \min x_i^{(0)}(k)} \tag{1}$$

2. The-lower-the-better (LB)

$$x_i^*(k) = \frac{\max x_i^{(0)}(k) - x_i^{(0)}(k)}{\max x_i^{(0)}(k) - \min x_i^{(0)}(k)} \tag{2}$$

3. The-nominal-the-better (NB)

$$x_i^*(k) = 1 - \frac{\left|x_i^{(0)}(k) - x^{(0)}\right|}{\max x_i^{(0)}(k) - x^{(0)}} \tag{3}$$

where $x_i^*(k)$ is the generating value obtained from gray relational analysis; $\min x_i^{(0)}(k)$ is the minimum value of sequence $x_i^{(0)}(k)$; $\max x_i^{(0)}(k)$ is the maximum value of sequence $x_i^{(0)}(k)$; and $x^{(0)}$ is the desired value.

2.3.2 Gray relational coefficient

The gray relational coefficient is determined to express the relationship between ideal and actual normalized experimental data. In addition, the gray relational coefficient can be calculated as

$$\gamma\left(x_0(k), x_i^*(k)\right) = \frac{\Delta\min + \zeta \cdot \Delta\max}{\Delta_{0i}(k) + \zeta \cdot \Delta\max} \tag{4}$$

where $x_0(k)$ is the ideal sequence; $\Delta_{0i}(k) = \left|x_0(k) - x_i^*(k)\right|$ is the difference of the absolute value between $x_0(k)$ and $x_i^*(k)$; $\Delta\min = \forall j^{\min} \in i \forall k^{\min}\left|x_0(k) - x_j^*(k)\right|$ is the smallest value of Δ_{0i}; $\Delta\max = \forall j^{\max} \in i \forall k^{\max}\left|x_0(k) - x_j^*(k)\right|$ is the largest value of Δ_{0i}; and ζ is a distinguishing coefficient that is defined in the range between zero and one. Generally, the distinguishing coefficient can be adjusted to fit the practical requirements and it is normally set at 0.5.

2.3.3 Gray relational grade

The gray relational grade that is obtained by averaging the gray relational coefficients associated with each performance characteristic. It can be expressed as

$$\Gamma_i = \frac{1}{n}\sum_{i=1}^{n} \gamma\left(x_0(k), x_i^*(k)\right) \tag{5}$$

where n is the number of process responses.

Generally, a high value of the gray relational grade corresponds to a strong relational degree between the reference sequence $x_0(k)$ and the comparative sequence $x_i^*(k)$. As mentioned above, the reference sequence $x_0(k)$ is the best response of the experimental results. Therefore, a higher value of the gray relational grade means that the corresponding machining parameters are closer to the optimal levels. In other words, the optimization of machining parameters associated with the complex multiple performance characteristics can be converted into the optimal resolution of single gray relational grade.

2.3.4 Analysis of variance

The gray relational grades can be statistically studied by ANOVA to determine the effects of each machining parameter on the process responses and to elucidate which machining parameters significantly affected the process responses. The related equations are [35–39]:

$$S_m = \frac{(\sum y_{0i})^2}{18} \tag{6}$$

$$S_T = \sum y_{0i}^2 - S_m \tag{7}$$

$$S_A = \frac{\sum y_{0Ai}^2}{N} - S_m \tag{8}$$

$$S_E = S_T - \sum S_A \tag{9}$$

$$V_A = \frac{S_A}{f_A}, \tag{10}$$

$$C_A = \frac{V_A}{V_T} \times 100\% \tag{11}$$

where:

S_m sum of squares, based on the mean
S_T sum of squares, based on the total variation

S_A sum of squares, based on parameter A (for example, $A=P$, I_p, I_H, τ_P, V, and S_v)
S_E sum of squares, based on the error
y_{0i} value of y_0 in the ith experiment (i=1 to 18)
y_{0Ai} sum of the ith level of parameter A (i=1,2 or i=1,2,3)
N repeating number of each level of parameter A
f_A number of degrees of freedom of parameter A
V_A variance of parameter A
V_T sum of variance
C_A contribution degree of parameter A

Herein, the contribution of the input parameters was defined as significant if the calculated contribution C_A exceed 20%.

3 Results and discussion

3.1 Effects of magnetic-force-assisted EDM process

Figure 3 shows the discharge waveforms of magnetic-force-assisted EDM and the conventional EDM under two discharge energy levels (I_p, 5 A and τ_p, 20 μs; I_p, 20 A and τ_p, 350 μs) at an elapsed machining time of 5 min. Indeed, monitoring the discharge waveform can determine the stability of EDM process and inspect the state of gap condition. Several factors may deteriorate the discharge waveforms. Generally, increasing the number of abnormal discharge waveforms means that the machining efficiency of the EDM process is reduced. The machining debris accumulated on the machining gap and expelled ineffectively from the machining gap are the main factors that affected the gap condition leading to a poor machining efficiency. When the un-expelled machining debris that accumulated in the machining gap disturbs the dielectric recovery to the original isolated state, abnormal electrical discharge will be generated in the machining zone. As shown in Fig. 3, at the initial stage (5 min), the discharge waveforms were very good for both magnetic-force-assisted EDM and conventional EDM. Only a few of abnormal discharge waveforms were observed, and there was no significant difference between the two processes at this period.

Figure 4 shows the discharge waveforms obtained at 35 min of elapsed machining time. As shown in this figure, the

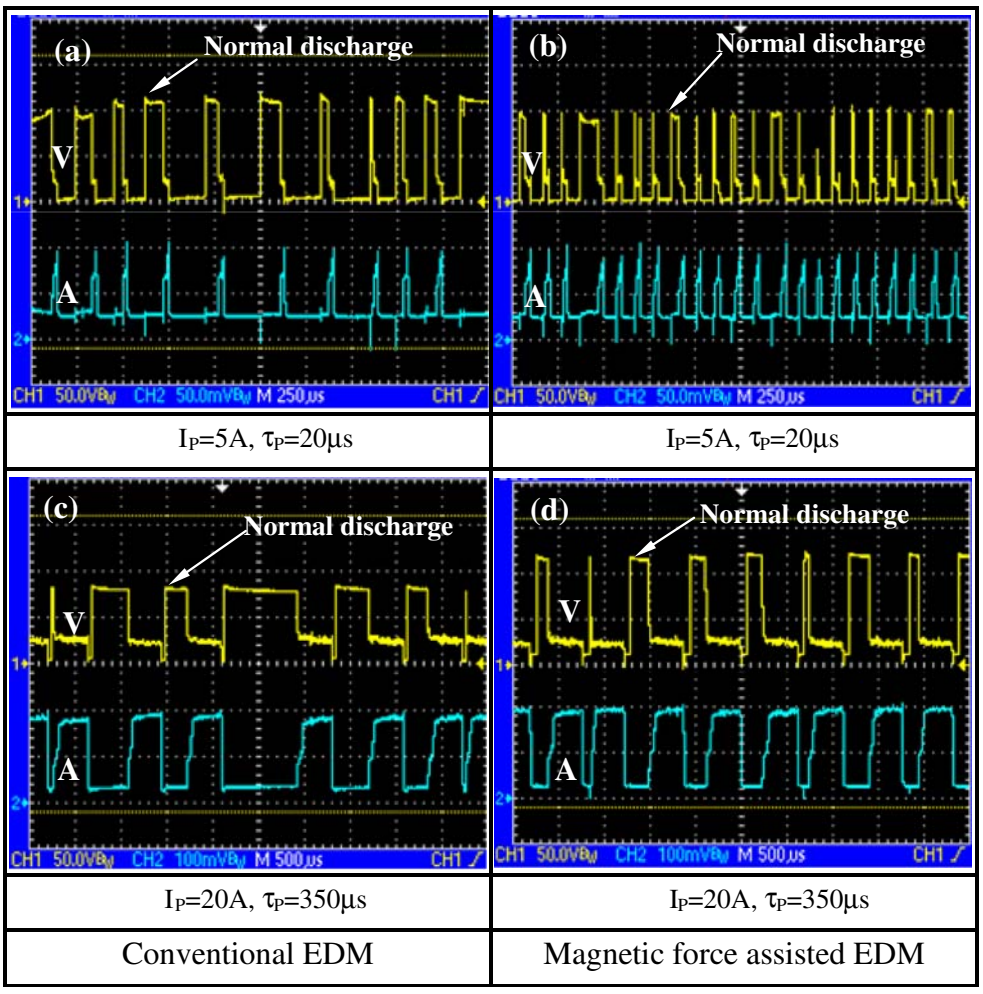

Fig. 3 Discharge waveforms of magnetic-force-assisted EDM and conventional EDM (after machining 5 min)

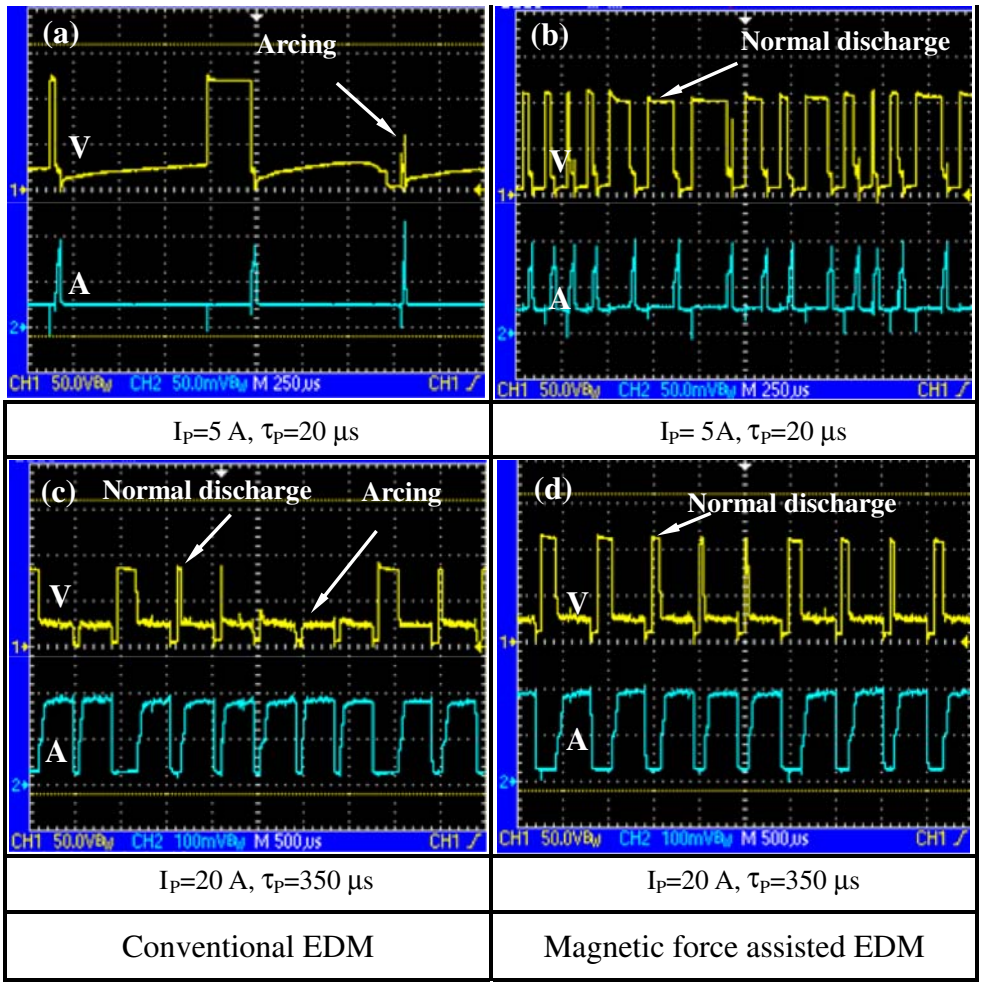

Fig. 4 Discharge waveforms of magnetic-force-assisted EDM and conventional EDM (after machining 35 min)

number of effective discharge waveforms obtained by magnetic-force-assisted EDM were more than that by conventional EDM. When the elapsed machining time prolonged to 35 min, the machining debris was increased, and the possibility of the machining debris to accumulate on the machining zone was also increased. Therefore, a large number of abnormal electrical discharge waveforms would be observed due to massive machining debris accumulated in the machining gap. The magnetic-force-assisted EDM could obviously reduce the adverse effect of accumulated debris. Since the abnormal electrical discharge was extensively reduced, the stability of EDM progress was maintained properly. Therefore, the magnetic-force-assisted EDM process significantly improved the machining efficiency.

Figure 5 shows a comparison of MRR and SR between the magnetic-force-assisted EDM and conventional EDM. According to the experimental results, the MRR of the magnetic-assisted EDM was near three times compared to conventional EDM, and the SR of the magnetic-force-assisted EDM was less than that of conventional EDM. When an assisted device of magnetic force was attached to the EDM machine, the debris would be driven by the assisted magnetic force to expel from the machining gap more easily and quickly, and the probability of abnormal discharge would be diminished. Therefore, the MRR of the EDM was facilitated by the assisted magnetic force. Moreover, the un-expelled debris accumulated on the machining zone would result in abnormal discharge and would re-melt to the machined surface, so the machined surface would be damaged and the recast layer would be thickened. As a result, the surface roughness obtained by conventional EDM was higher than that by the magnetic-force-assisted EDM.

Figure 6 shows the SEM micrographs of the magnetic-force-assisted EDM and conventional EDM under low- and high-discharge energy levels. As shown in this figure, the discharge craters on the machined surface obtained at higher discharge energy was deeper and larger than that at lower discharge energy level. Moreover, the topographies of the machined surface obtained by conventional EDM were coarser than that by the magnetic-force-assisted EDM not only under low-discharge energy level (I_p, 5 A; τ_p, 20 μs) but also under high situation (I_p, 20 A; τ_p, 350 μs).

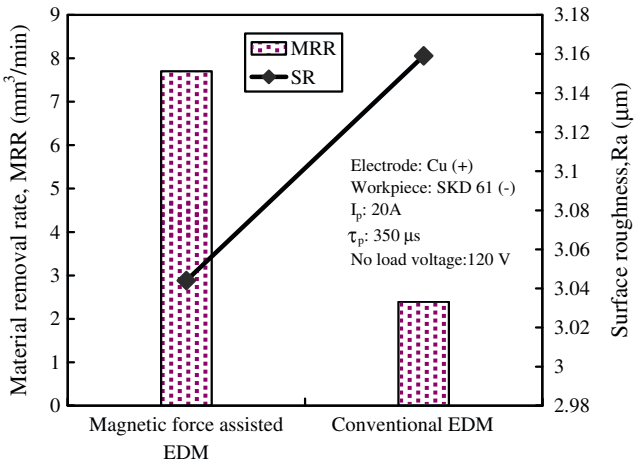

Fig. 5 Comparison of MRR and SR between magnetic-force-assisted EDM and conventional EDM

This can be explained based on the fact that the machining debris would not be ejected completely using conventional EDM. A thicker recast layer was formed and the surface topography became coarser, since melting of unremoved workpiece materials would re-solidify and adhere on the machined surface. In contrast, the assisted magnetic force could facilitate and drive the machining debris expelled from the machining gap easily and quickly. The topographies of the machined surface were more even and clean due to less globules of debris. Thus, the topographies obtained by the magnetic-force-assisted EDM were even and fine.

Some melting materials were not flushed away completely by the dielectric fluid from the machined surface during EDM process. The surplus material was removed by the EDM removal mechanisms such as melting, vaporization, and dielectric explosion resulted from the electrical discharge within the discharge column. Consequently, the unflushed workpiece materials would re-solidify and deposit on the machined surface due to rapid cooling via dielectric fluid during the cease interval, and a recast layer would be formed on the machined surface. The recast layer contained workpiece, electrode, and dielectric compositions with high hardness and excellent corrosion resistance. Moreover, the formation of recast layer will be affected by EDM machining parameters. When the electrical discharge energy is set at large level, the machined surface gained a thicker recast layer. However, due to the violent temperature gradient during the cooling interval, the recast layer exhibited intensive surface cracks that worsened the fatigue strength, reliability, accuracy, and service life of the components fabricated using EDM process. Figure 7 shows the cross sections of the machined surfaces obtained by the

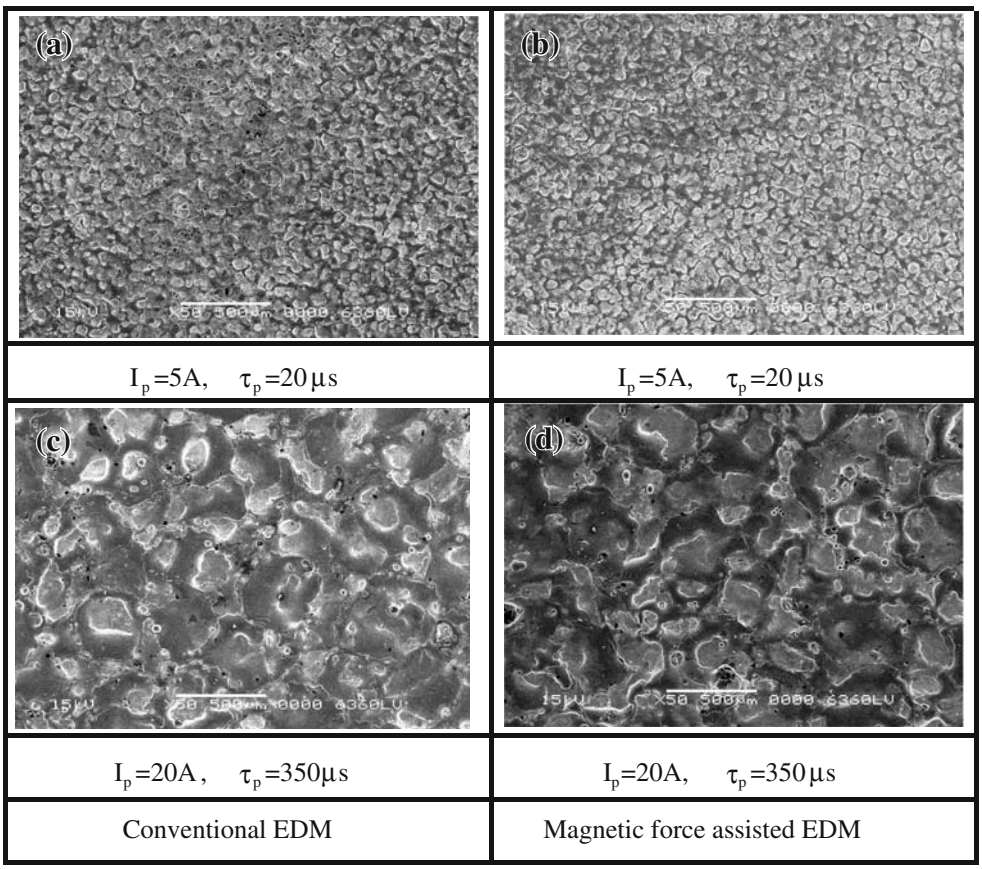

Fig. 6 Machined surface obtained by magnetic-force-assisted EDM and conventional EDM

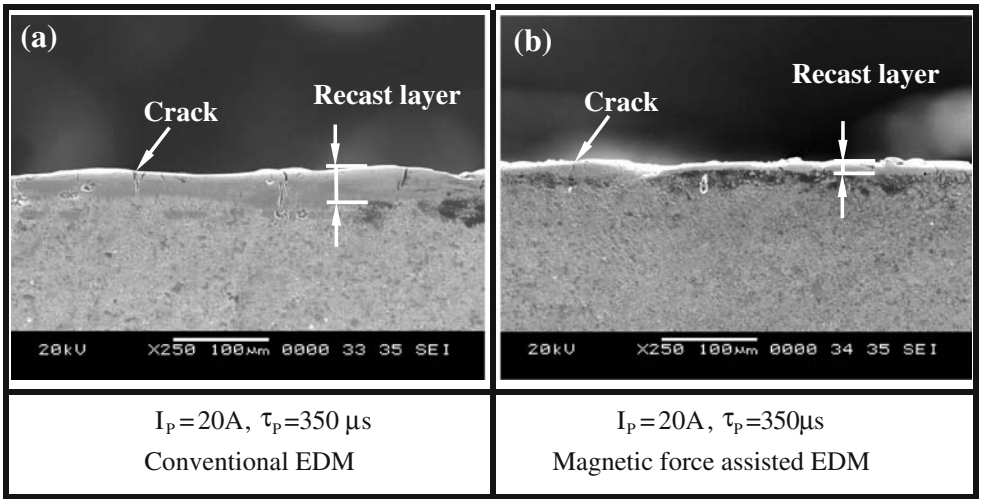

Fig. 7 Cross section of machined surface obtained by magnetic-force-assisted EDM and conventional EDM

magnetic-force-assisted EDM and conventional EDM under a peak current of 20 A and pulse duration of 350 μs. As shown in this figure, the recast layer thickness of conventional EDM was thicker than that of magnetic-force-assisted EDM. It can be attributed to the fact that enormous amount of unexpelled debris would be re-melted and re-solidified to deposit on the machined surface, and then a thicker recast layer would be formed in the conventional EDM process. In this figure, it can be seen that the surface cracks on the machined surface are obtained not only through the conventional EDM but also through magnetic-force-assisted EDM. Moreover, the surface cracks obtained by the magnetic-force-assisted EDM were shorter and narrower than that by conventional EDM. The surface cracks extended to the bottom of the recast layer and revealed a trend that is perpendicular to the machined surface. Therefore, the magnetic-force-assisted EDM exhibited beneficial effects on the surface integrity, which revealed not only smaller recast layer thickness but also less surface cracks.

3.2 Gray relational analysis for magnetic-force-assisted EDM process

Gray relational analysis associated with Taguchi experimental design method is a new approach to optimize the machining parameters of a versatile process with multiple performance characteristics. In this work, the gray relational analysis was adopted to evaluate the multiple performance characteristics of MRR, EWR, and SR for a novel process

Table 5 L18 orthogonal array, control parameters and observed values

Number	Control parameters								Observed values		
	P	I_p	I_H	τ_p	V	S_v	e1	e2	MRR (mm^3/min)	EWR (mm^3/min)	SR (Ra/μm)
1	(−)	5	0.4	50	120	10	1	1	0.1245	0.0515	1.4975
2	(−)	5	0.8	150	160	20	2	2	0.1817	0.0622	1.4350
3	(−)	5	1.2	460	200	40	3	3	0.2486	0.0470	1.7594
4	(−)	10	0.4	50	160	20	3	3	4.7538	0.0685	1.5907
5	(−)	10	0.8	150	200	40	1	1	9.7917	0.0400	2.4445
6	(−)	10	1.2	460	120	10	2	2	11.4074	0.0283	1.4362
7	(−)	20	0.4	150	120	40	2	3	35.6823	0.0530	4.0057
8	(−)	20	0.8	460	160	10	3	1	41.9140	0.0068	2.7110
9	(−)	20	1.2	50	200	20	1	2	16.1047	0.0964	3.7215
10	(+)	5	0.4	460	200	20	2	1	0.1323	0.0590	1.3160
11	(+)	5	0.8	50	120	40	3	2	0.0501	0.0645	1.4960
12	(+)	5	1.2	150	160	10	1	3	0.0838	0.0552	1.2560
13	(+)	10	0.4	150	200	10	3	2	1.6708	0.0651	1.2607
14	(+)	10	0.8	460	120	20	1	3	2.0777	0.0445	1.2795
15	(+)	10	1.2	50	160	40	2	1	2.4436	0.0772	1.4833
16	(+)	20	0.4	460	160	40	1	2	3.2042	0.1359	1.7312
17	(+)	20	0.8	50	200	10	2	3	2.9708	0.5891	1.8855
18	(+)	20	1.2	150	120	20	3	1	2.2503	0.2200	1.6872

of the magnetic-force-assisted EDM. Furthermore, an optimization of machining parameters was obtained according to receiving a higher gray relational grade. In other words, the gray relational grade was treated as the overall evaluation of experimental data for the multiple performance characteristics. Table 5 lists the L18 orthogonal array, control parameters, and observed experimental values. The experiments were conducted to optimize the machining parameters of the magnetic-force-assisted EDM through gray relational analysis. The values of gray relational generating associated with each experimentally observed value and the ideal sequence are shown in Table 6. In this work, the MRR is desired to obtain a higher value, namely, the-higher-the-better (HB) feature, and the EWR and SR also exhibit the feature of the-lower-the-better (LB) feature. Consequently, the gray relational coefficients can be calculated from the gray relational generating. After averaging the corresponding gray relational coefficients, the gray relational grades were obtained. Table 7 presents the results of gray relational coefficients, gray relational grades, and their ranks. The results show that experiment number 8 has the largest gray relational grade. It can be expected that the levels of each machining parameter are superior to attain a better multiple performance characteristics.

Table 7 Gray relational coefficients and grades

Number	Gray relational coefficient			Gray relational grade	
	MRR	EWR	SR	Value	Rank
1	0.3337	0.8669	0.8506	0.6837	8
2	0.3340	0.8400	0.8848	0.6863	7
3	0.3344	0.8786	0.7320	0.6483	13
4	0.3603	0.8252	0.8042	0.6633	11
5	0.3945	0.8976	0.5363	0.6095	14
6	0.4069	0.9313	0.8841	0.7408	2
7	0.7706	0.8631	0.3333	0.6557	12
8	1	1	0.4858	0.8286	1
9	0.4478	0.7646	0.3580	0.5235	17
10	0.3338	0.8480	0.9582	0.7133	6
11	0.3333	0.8346	0.8514	0.6731	9
12	0.3335	0.8574	1	0.7303	4
13	0.3422	0.8331	0.9966	0.7239	5
14	0.3445	0.8853	0.9832	0.7377	3
15	0.3465	0.8054	0.8581	0.6700	10
16	0.3510	0.6928	0.7431	0.5956	15
17	0.3496	0.3333	0.6859	0.4563	18
18	0.3454	0.5772	0.7612	0.5613	16

3.3 ANOVA and optimal machining parameters

Statistical analysis of ANOVA was adopted to evaluate the machining parameters, which significantly affected the multiple performance characteristics. Table 8 presents the ANOVA results of the gray relational grades obtained by the magnetic-force-assisted EDM. Besides, the contribution (C_A) is also listed to assess the significant parameters. When the ratio of contribution (C_A) exceeded 20% of the sum of variance, the correlated machining parameter was regarded as the significant parameter. As shown in Table 8, peak current (I_p), pulse duration (τ_p), and no-load voltage (V) were the significant machining parameters that obviously influenced the multiple performance characteristics of the magnetic-force-assisted EDM process. Table 9 shows the response of the gray relational grades associated with the levels of each machining parameter and the effects of each machining parameter. In addition, the response graph of the gray relational grades is shown in Fig. 8. From the analysis of results presented in Table 9 and Fig. 8, the optimal combinational levels of machining parameters associated with multiple performance characteristics from the magnetic-force-assisted EDM process are as follows: negative machining polarity (P), 10 A peak current (I_p), 0.4 A auxiliary current with high voltage (I_H), 460 μs pulse duration (τ_p), 160 V no-load voltage (V), and 10 V servo reference voltage (S_v).

Table 6 Gray relational generating of MRR, EWR, and SR

Number	MRR	EWR	SR
	Ideal sequence		
	1	1	1
1	0.0018	0.9232	0.9122
2	0.0031	0.9048	0.9349
3	0.0047	0.9309	0.8169
4	0.1124	0.8941	0.8783
5	0.2327	0.9430	0.5678
6	0.2713	0.9631	0.9345
7	0.8511	0.9207	0
8	1	1	0.4709
9	0.3835	0.8461	0.1034
10	0.0020	0.9104	0.9782
11	0	0.9009	0.9127
12	0.0008	0.9168	1
13	0.0387	0.8998	0.9983
14	0.0484	0.9352	0.9915
15	0.0572	0.8792	0.9173
16	0.0753	0.7783	0.8272
17	0.0698	0	0.7711
18	0.0526	0.6338	0.8432

3.4 Confirmation experiment

The optimal combination levels of machining parameters associated with multiple performance characteristics were

Table 8 ANOVA of the gray relational grades

Parameter (A)	Degree (f_A)	Square sum (S_A)	Variance (V_A)	Contribution, % (C_A)
P	1	0.0018	0.0018	3.2
I_p	2	0.0300	0.0150	27.4[a]
I_H	2	0.0023	0.0012	2.1
τ_p	2	0.0295	0.0147	26.9[a]
V	2	0.0226	0.0113	20.7[a]
S_v	2	0.0098	0.0049	8.9
E_{e1+e2}	6	0.0353	0.0059	10.8
Total	17	0.1311		100

[a] Significant parameter: Contribution ≧20%

determined and confirmed as follows. The estimated gray relational grade is calculated as

$$\Gamma = \overline{\Gamma}_m + \sum_{i=1}^{n_o} \left(\overline{\Gamma}_i = \overline{\Gamma}_m\right) \tag{12}$$

Γ estimated gray relational grade for optimal combination levels of machining parameters
$\overline{\Gamma}_m$ total mean gray relational grade
n_0 the number of significant parameters
$\overline{\Gamma}_i$ mean gray relational grade at the optimal level

Table 10 displays the results of the confirmation experiments. This table indicates that MRR is increased from 8.2417 to 15.5312 mm^3/min, EWR is reduced from 0.0535 to 0.0323 mm^3/min, and SR is improved from 2.25 to 1.33 μm when the machining parameters are set at the optimal levels. The initial conditions are set as follows: P (−), I_p(10 A), I_H(0.8 A), τ_p (150 μs), V (160 V), and S_v (20 V). Moreover, the gray relational grade for multiple performance characteristics in the magnetic-force-assisted EDM process was greatly improved (from 0.6085 to 0.7702). Therefore, the experimental results confirm that the machining parameters of the magnetic-force-assisted EDM could be optimized for multiple performance characteristics through gray relational analysis.

Table 9 Response table for gray relational grades

Symbol	Parameter	Level 1	Level 2	Level 3	Max–min
A	P	0.6711	0.6513		0.0198
B	I_p	0.6892	0.6909	0.6035	0.0874
C	I_H	0.6726	0.6652	0.6457	0.0269
D	τ_p	0.6116	0.6612	0.7107	0.0991
E	V	0.6754	0.6957	0.6125	0.0832
F	S_v	0.6939	0.6476	0.5428	0.0519

Mean value of the gray relational grade=0.6612

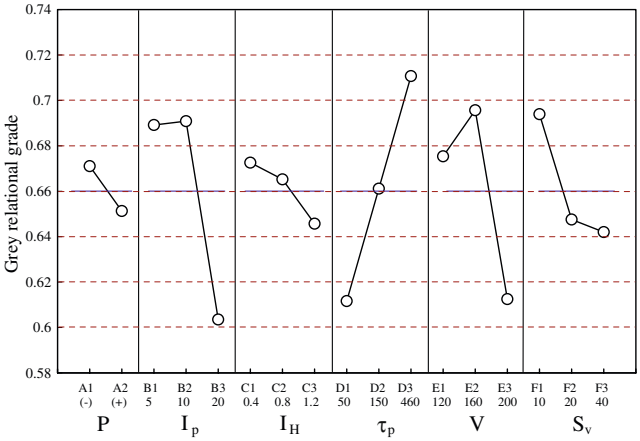

Fig. 8 Response graph of gray relational grade

4 Conclusions

The effects of the novel process of magnetic-force-assisted EDM were explored, and the optimizing machining parameters associated with multiple performance characteristics of magnetic-force-assisted EDM was determined using gray relational analysis. From the experimental results and statistical analysis of ANOVA, the following conclusions have been drawn.

1. The number of effective discharge waveforms obtained by magnetic-force-assisted EDM was more than that by conventional EDM. Thus, the stability of EDM process and the machining efficiency were improved with the magnetic-force-assisted EDM process. Consequently, the MRR of the magnetic-assisted EDM was near three times compared to conventional EDM, and the SR of the magnetic-force-assisted EDM was less than that of conventional EDM.
2. The topography of the machined surface was smoother than that of conventional EDM. Moreover, the thickness of recast layer and the surface cracks on the

Table 10 Results of the confirmation experiment

Observer values	Initial levels of machining parameters	Optimal combination levels of machining parameters	
		Prediction	Experiment
Setting level	$A_1B_2C_2D_2E_2F_2$	$A_1B_1C_2D_3E_2F_1$	$A_1B_1C_2D_3E_2F_1$
MRR	8.2417	–	15.5312
EWR	0.0535	–	0.0323
SR	2.25	–	1.33
Gray relational grade	0.6085	0.7749	0.7702

machined surface were significantly reduced in the magnetic-force-assisted EDM process.

3. ANOVA results indicated that the peak current (I_p), pulse duration (τ_p), and no-load voltage (V) were the significant machining parameters that obviously affected the multiple performance characteristics in the magnetic-force-assisted EDM process. Moreover, the optimal combinational levels of machining parameters associated with multiple performance characteristics in the magnetic-force-assisted EDM process are as follows: negative machining polarity (P), 10 A peak current (I_p), 0.4 A auxiliary current with high voltage (I_H), 460 μs pulse duration (τ_p), 160 V no-load voltage (V), and 10 V servo reference voltage (S_v).
4. The machining parameters of magnetic-force-assisted EDM could be optimized for multiple performance characteristics. Moreover, MRR, EWR, and SR were greatly improved when the machining parameters were set at the optimal levels.

Acknowledgment The authors would like to thank the National Science Council of the Republic of China, Taiwan, for financially supporting this research under Contract No. NSC 92-2212-E-235-005.

References

1. Fallbohmer P, Altan T, Tonshoff HK, Nakagawa T (1996) Survey of the die and mold manufacturing industry. J Mater Process Technol 59:158–168 doi:10.1016/0924-0136(96)02297-2
2. Khairy AB (2001) Aspects of surface and edge finish by magnetoabrasive particles. J Mater Process Technol 116:77–83 doi:10.1016/S0924-0136(01)00840-8
3. Chang GW, Yan BH, Hsu RT (2002) Study on cylindrical magnetic abrasive finishing using unbonded magnetic abrasives. Int J Mach Tools Manuf 42:575–583 doi:10.1016/S0890-6955(01)00153-5
4. Singh S, Shan HS (2002) Development of magneto abrasive flow machining process. Int J Mach Tools Manuf 42:953–959 doi:10.1016/S0890-6955(02)00021-4
5. Mori T, Hirota K, Kawashima Y (2003) Clarification of magnetic abrasive finishing mechanism. J Mater Process Technol 143–144:682–686 doi:10.1016/S0924-0136(03)00410-2
6. Kim JD (2003) Polishing of ultra-clean inner surfaces using magnetic force. Int J Adv Manuf Technol 21:91–97
7. Yin S, Shinmura T (2004) A comparative study: polishing characteristics and its mechanisms of three vibration models in vibration-assisted magnetic abrasive polishing. Int J Mach Tools Manuf 44:383–390 doi:10.1016/j.ijmachtools.2003.10.002
8. Yan BH, Chang GW, Chang JH, Hsu RT (2004) Improving electrical discharge machined surfaces using magnetic abrasive finishing. Machg Sci Technol 8(1):103–118 doi:10.1081/MST-120034246
9. Wang Y, Hu D (2005) Study on the inner surface finishing of tubing by magnetic abrasive finishing. Int J Mach Tools Manuf 45:43–49 doi:10.1016/j.ijmachtools.2004.06.014
10. Jayswal SC, Jain VK, Dixit PM (2005) Modeling and simulation of magnetic abrasive finishing process. Int J Adv Manuf Technol 26:477–490 doi:10.1007/s00170-004-2180-x
11. Singh DK, Jain VK, Raghuram V (2006) Experimental investigations into forces acting during a magnetic abrasive finishing process. Int J Adv Manuf Technol 30:652–662 doi:10.1007/s00170-005-0118-6
12. Lin CT, Yang LD, Chow HM (2007) Study of magnetic abrasive finishing in free-form surface operations using the Taguchi method. Int J Adv Manuf Technol 34:122–130 doi:10.1007/s00170-006-0573-8
13. Kim JD, Jin DX, Choi MS (1997) Study on the effect of a magnetic field on an electrolytic finishing process. Int J Mach Tools Manuf 37:401–408 doi:10.1016/S0890-6955(96)00071-5
14. De Bruijn HE, Delft TH, Pekelharig AJ (1978) Effect of a magnetic field on the gap cleaning in EDM. Ann CIRP 27(1):93–95
15. Rajurkar KP, Pandit SM (1988) Formation and ejection of EDM debris. Trans ASME 108(2):22–26
16. Masuzawa T, Cui X, Taniguchi N (1992) Improved jet flushing for EDM. Ann CIRP 41:239–242
17. Soni JS (1994) Microanalysis of debris formed during rotary EDM of titanium alloy (Ti6 Al 4V) and die steel (T215 Cr12). Wear 177:71–79 doi:10.1016/0043-1648(94)90119-8
18. Lou YF (1997) The dependence of interspace discharge transitivity upon the gap debris in precision electrodischarge machining. J Mater Process Technol 68:121–131 doi:10.1016/S0924-0136(96)00019-2
19. Cetin S, Okada A, Uno Y (2004) Effect of debris accumulation on machining speed in EDM. Int J Electr Mach 9:9–14
20. Kremer D, Lhiaubet C, Moisan A (1991) A study of the effect of synchronizing ultrasonic vibrations with pulse in EDM. Ann CIRP 40(1):211–214
21. Thoe TB, Aspinwall DK, Killey N (1999) Combined ultrasonic and electrical discharge machining of ceramic coated nickel alloy. J Mater Process Technol 92–93:323–328 doi:10.1016/S0924-0136(99)00117-X
22. Lin YC, Yan BH, Chang YS (2000) Machining characteristics of titanium alloy (Ti-6Al-4V) using combination process of EDM with USM. J Mater Process Technol 104:171–177 doi:10.1016/S0924-0136(00)00539-2
23. Zhang QH, Zhang JH, Deng JX, Qin Y, Niu ZW (2002) Ultrasonic vibration electrical discharge machining in gas. J Mater Process Technol 129:135–138 doi:10.1016/S0924-0136(02)00596-4
24. Lin YC, Yan BH, Huang FY (2001) Surface modification of Al-Zn-Mg aluminum alloy using combined process of EDM with USM. J Mater Process Technol 115:359–366 doi:10.1016/S0924-0136(01)01017-2
25. Lin CL, Lin JL, Ko TC (2002) Optimisation of the EDM process based on the orthogonal array with fuzzy logic and grey relational analysis method. Int J Adv Manuf Technol 19:271–277 doi:10.1007/s001700200034
26. Lin JL, Lin CL (2002) The use of the orthogonal array with grey relational analysis to optimize the electrical discharge machining process with multiple performance characteristics. J Mache Tools Manuf 42:237–244 doi:10.1016/S0890-6955(01)00107-9
27. Wang CH, Tong LI (2003) Quality improvement for dynamic ordered categorical response using grey relational analysis. Int J Adv Manuf Technol 21:377–383 doi:10.1007/s001700300043
28. Jeyapaul R, Shahabudeen P, Krishnaiah K (2003) Quality management research by considering multi-response problems in the Taguchi method—a review. Int J Adv Manuf Technol 21:377–383 doi:10.1007/s001700300043
29. Kao PS, Hocheng H (2003) Optimization of electrochemical polishing of stainless steel by grey relational analysis. J Mater Process Technol 140:255–259 doi:10.1016/S0924-0136(03)00747-7
30. Huang JT, Liao YS (2003) Optimization of machining parameters of wire-EDM based on grey relational and statistical analyses. Int J Prod Res 41(8):1707–1720 doi:10.1080/1352816031000074973

31. Singh PN, Raghukandan K, Pai BC (2004) Optimization by grey relational analysis of EDM parameters on machining Al-10% SiCp composites. J Mater Process Technol 155–156:1865–1661
32. Lin JL, Lin CL (2005) The use of grey-fuzzy logic for the optimization of the manufacturing process. J Mater Process Technol 160:9–14 doi:10.1016/j.jmatprotec.2003.11.040
33. Pan LK, Wang CC, Wei SL, Sher HF (2007) Optimizing multiple quality characteristics via Taguchi method-based grey analysis. J Mater Process Technol 182:107–116 doi:10.1016/j.jmatprotec.2006.07.015
34. Gangadhar A, Shunmugam MS, Philip PK (1992) Pulse train studies in EDM with controlled pulse Relaxation. Int J Mach Tools Manuf 32(5):651–657 doi:10.1016/0890-6955(92)90020-H
35. Liao YS, Huang JT, Su HC (1997) A study on the machining-parameters optimization of wire electrical discharge machining. J Mater Process Technol 71:487–493 doi:10.1016/S0924-0136(97)00117-9
36. Lin YC, Yan BH, Huang FY (2001) Surface improvement using a combination electrical discharge machining with ball burnish machining based on the Taguchi method. Int J Adv Manuf Technol 18:673–682 doi:10.1007/s001700170028
37. Lin YC, Cheng CH, Su BL, Hwang LR (2006) Machining characteristics and optimization of machining parameters of SKH 57 high-speed-steel using electrical-discharge-machining based on Taguchi method. Mater Manuf Process 21:922–929 doi:10.1080/03602550600728133
38. Phadke MS (1989) Quality engineering using robust design. Prentice Hall, Englewood Cliffs, NJ
39. Tzeng HJ, Yan BH, Hsu RT, Chow HM (2007) Finishing effect of abrasive flow machining on micro slit fabricated by wire-EDM. Int J Adv Manuf Technol 34:649–656 doi:10.1007/s00170-006-0632-1